OXFORD | **SOT** | **Society of Toxicology**
www.toxsci.oxfordjournals.org

Exposure to CrVI during Early Pregnancy Increases Oxidative Stress and Disrupts the Expression of Antioxidant Proteins in Placental Compartments

Sakhila K. Banu,[1] Jone A. Stanley, Kirthiram K. Sivakumar, Robert J. Taylor, Joe A. Arosh, and Robert C. Burghardt

Department of Veterinary Integrative Biosciences, College of Veterinary Medicine and Biomedical Sciences, Mail stop TAMU 4458, Texas A&M University, College Station, Texas 77843

[1]To whom correspondence should be addressed at Department of Integrative Biosciences, College of Veterinary Medicine and Biomedical Sciences, Texas A&M University, College Station, Texas 77843. Fax: 979-847-8981. E-mail: skbanu@cvm.tamu.edu.

ABSTRACT

Epidemiologic studies document relationships between chromium VI (CrVI) exposure and increased risk of spontaneous abortion, stillbirth, preterm birth, and neonatal death in pregnant women. Environmental contamination with CrVI is a growing problem both in the United States and developing countries. CrVI is widely used in numerous industries. This study was designed to understand the mechanism of CrVI toxicity on placental oxidative stress and antioxidant (AOX) machinery. Pregnant mother rats were treated with or without CrVI (50 ppm $K_2Cr_2O_7$) through drinking water from gestational day (GD) 9.5–14.5, and placentas were analyzed on GD 18.5. Results indicated that CrVI reduced the trophoblast cell population. CrVI increased reactive oxygen species (ROS) and decreased the expression of AOX proteins. CrVI disrupts the trophoblast proliferation of the placenta. This study provides insight into the critical role of AOXs in placental function.

Key words: trophoblast; rat placenta and chromium; oxidative stress; Gpx1; Sod; Prdx3.

According to the September 2016 report by the Environmental Working Group, analysis of federal data from nationwide drinking water tests shows that hexavalent chromium (CrVI) contaminates water supplies for more than 200 million Americans in all 50 states (Andrews, 2016). Environmental contamination with CrVI and the associated health effects of CrVI exposure in humans is a growing problem in the Unite States. The USEPA approved safety limit for Cr levels in drinking water is 0.1 ppm (USEPA, 2009). A series of epidemiological studies, examining women who work in chromium industries such as tanneries and leather industries, have indicated that prenatal exposure to CrVI through the mother resulted in high Cr levels in maternal blood, urine, umbilical cord and placental tissue (Li *et al.*, 2008; Shmitova, 1980), resulting in spontaneous abortion, preterm labor (Hemminki *et al.*, 1983; Yang *et al.*, 2013), developmental defects (Das and Mishra, 2008; Stern *et al.*, 1986), intrauterine growth restriction (IUGR) and low birth weight (Quansah and Jaakkola, 2008).

CrVI has been used in numerous industries such as leather and textiles, metallurgical, chemical and automobile (Banu, 2013; Barceloux, 1999). Due to increased use and improper disposal of CrVI, levels in the water, soil and air continue to increase (Pellerin and Booker, 2000; Shanker and Venkateswarlu, 2011). Epidemiological studies have reported frequent health problems in CrVI-exposed populations, that include cancer, dermatitis, asthma, chronic bronchitis, hypertension, chromosomal abrasions, back pain, metabolic syndrome, hemoglobin changes, and DNA damage in lymphocytes (Junaid *et al.*, 2016). Approximately, 300 000 workers are severely affected by the Cr compounds annually around the globe (Annangi *et al.*, 2016). Health implications due to exposure to toxic heavy metals, including Cr in the environment have risen in recent years (Annangi *et al.*, 2016; Jomova and Valko, 2011; Notarachille *et al.*, 2014; Valko *et al.*, 2005). Therefore, Cr and other heavy metals associated with health implications in exposed workers are a matter of great concern.

Placenta is the interface between mothers and developing embryos/fetuses that performs a number of critical functions throughout gestation (Lewis et al., 2012). The placenta facilitates the exchange of metabolites between mother and fetus. Pregnancy-associated diseases such as preeclampsia and IUGR affect up to 10% of pregnancies (Walentin et al., 2015). Placenta plays an important role as the gateway for the entry of Endocrine Disrupting Chemicals (EDCs) into the fetal environment. Therefore, it is an important organ for the evaluation of risks for mothers and embryos/fetuses in toxicity screening. Mechanistic evaluation of placental toxicity has been scarce and/or incomplete in experimental animals. Rat placental models have been useful for evaluating adverse effects of EDCs that affect human reproductive development since there are several similarities (despite differences) between rats and humans in early placental development (Ain et al., 2006; Fonseca et al., 2012). Both rat and human placenta are hemochorial and share some unique features regarding uterine trophoblast invasion and spiral artery remodeling (De Rijk et al., 2002; Soares et al., 2012).

A recent review suggested that higher level of Cr exposure in industrial workers results in high levels of the oxidative stress and hydroxyl radical generation in tissue-level compartments (Junaid et al., 2016). Oxidative stress is described as an imbalance in the production of reactive oxygen species (ROS) and the ability of antioxidant (AOX) defenses to scavenge them (Sies, 1997). It can arise from increased production of ROS and/or a decrease in AOX capacity (Myatt, 2010). Heavy metals are known to induce excessive production of ROS and decrease AOX levels in the placenta (Ahamed et al., 2009; Gundacker and Hengstschlager, 2012; Singh et al., 2015). Increased ROS is associated with impaired placental development and pathologic pregnancies, such as those complicated by preeclampsia and/or IUGR, by overloading AOX defenses with deleterious outcome (Myatt, 2010). Although much progress is being made in understanding the molecular pathways in placenta involved in the pathophysiologic pregnancy-related disorders, understanding the role of heavy metals in causing such disorders is unknown. Therefore, it is imperative to develop mechanistic research to understand metabolic pathways connecting heavy metal-induced oxidative stress, and AOX imbalance, and placental pathogenesis. Our recent studies have shown that gestational exposure to CrVI resulted in increased trophoblast cell (TC) apoptosis mediated through caspase-3/AIF/p53 pathways, and decreased TC survival mediated through a down regulation of XIAP, Bcl2 and Bcl-XL in a spatio-temporal manner (Banu et al., 2016).

Exposure of pregnant rats to CrVI through drinking water resulted in Cr accumulation in placental tissue (Sivakumar et al., 2014). CrVI rapidly passes through cells by anionic transporters (Ottenwaelder et al., 1988) and is readily converted in cells and biological fluids into CrIII by AOXs such as ascorbic acid, glutathione, N-acetyl cysteine, and AOX enzymes such as glutathione peroxidase (Gpx), superoxide dismutase (Sod), and catalase (Cat) (Liu and Shi, 2001). During this cellular reduction process, enormous amounts of ROS are generated, that increase oxidative stress. Therefore, determining the mechanism of CrVI-induced oxidative damage and/or AOX imbalance on placenta is imperative to identify strategies to mitigate adverse effects on fetal development. In addition, while IUGR and preterm labor is a predominant health issue in women exposed to CrVI, the underlying mechanisms are not well understood. Therefore, we hypothesize that "maternal exposure to CrVI during early pregnancy increases oxidative stress and causes an AOX imbalance, resulting in the reduction of the trophoblast population in placental compartments". The objectives of this investigation were to determine the effects of CrVI exposure on: (1) various TC lineages in placental compartments; (2) oxidative stress; and (3) endogenous AOX enzyme expression and activity in the placenta.

TABLE 1. Antibody Table (Source, Catalog Numbers, Dilutions, Host Species, and antigen sequences

S. No.	Peptide/Protein Target	Antigen sequence/Immunogen	Name of Antibody	Manufacturer; catalog no.	Species Raised in	Dilution Used
1	Cytokeratin	Cytokeratin isolated from bovine muzzle epidermis.	Rabbit Anti- Cytokeratin	Abcam; Ab9377	Rabbit polyclonal	1:50
2	CYP11A1	A synthetic peptide corresponding to a region of Human CYP11A1	Rabbit Anti-CYP11A1	Abcam; Ab75497	Rabbit polyclonal	1:1000
3	p57Kip2	Synthetic peptide (Human)	Rabbit Anti- p57 Kip2	Abcam; Ab4058	Rabbit polyclonal	1:200
4	FABP3	Synthetic peptide conjugated to KLH derived from within residues 100 - 200 of Human Cardiac FABP.	Rabbit Anti-FABP3	Abcam; Ab45966	Rabbit polyclonal	1:4000
5	Perforin	Immunogen corresponding to Human Perforin aa 280-555	Rabbit Anti-Perforin	Abcam; Ab180773	Rabbit polyclonal	1:200
6	Cyclin D1	Synthetic peptide corresponding to Human Cyclin D1 (C terminal)	Rabbit Anti-Cyclin-D1	Abcam; Ab16663	Rabbit polyclonal	1:100
7	Gpx1	Synthetic peptide within human glutathione peroxidase-1 aa 150 to the C-terminus (internal sequence).	Rabbit Anti-GPx1	Abcam; Ab108427	Rabbit monoclonal	1:100
8	SOD1	Synthetic peptide corresponding to residues near the amino- terminus of human SOD1	Rabbit anti-SOD1	Cell Signaling; 2770	Rabbit polyclonal	1:25
9	SOD2	Full length protein (Human).	Rabbit Anti-SOD2	Abcam; Ab13533	Rabbit polyclonal	1:500
10	PRDX3	Synthetic peptide conjugated to KLH derived from within residues 200 to the C-terminus of Human Prdx 3.	Rabbit Anti-PRDX3	Abcam; Ab73349	Rabbit polyclonal	1:100
11	TXN2	Recombinant full length protein (Human).	Mouse Anti-TXN2	Abcam; Ab16857	Mouse Monoclonal	1:100

MATERIALS AND METHODS

Chemicals. Reagents used in this study were purchased from Sigma-Aldrich, St Louis, Missouri or Thermo Fisher Scientific Inc., Austin, Texas. Details of sources of antibodies, catalog numbers, dilutions, host species, immunogens, and antigen sequences are given in the Table 1.

Animals. Timed pregnant Sprague-Dawley rats were purchased from Charles River Laboratories, Houston, Texas and maintained in AAALAC-approved animal facilities with a 12 h light/12 h dark regime at 23–25 °C, and provided with Teklad 4% mouse/rat diet and water ad libitum. Animal Use Protocols were performed in accordance with the NIH Guidelines for the Care and Use of Laboratory Animals, and with the standards established by Guiding Principles in the Use of Animals in Toxicology and specific guidelines and standards of the Society for the Study of Reproduction, and approved by the Animal Care and Use Committee of Texas A&M University.

In vivo dosing and experimental design. The *in vivo* CrVI dosing used in this investigation was chosen based on Cr levels in drinking water in highly polluted regions in developing countries that range from 19–50 ppm (Armienta-Hernandez and Rodríguez-Castillo, 1995; Dubey et al., 2001a; Rao et al., 2011; Sharma et al., 2012). The pregnancy dating system was determined as follows: Fertility-proven normal male rats were co-habited with female rats in the evening. The female rats were observed for vaginal plug and presence of sperm in the vaginal lavage the following day morning. Females that showed the presence of a vaginal plug and sperm in the vaginal lavage were marked as pregnancy day 0.5 or 0.5 day(s) postcoitum (dpc). Timed pregnant rats were divided into 2 groups: (1) Control (n = 10): rats received regular drinking water; (2) CrVI treatment (n = 5): rats received potassium dichromate (CrVI, 50 ppm) dissolved in drinking water from dpc 9.5–14.5. On gestational day (GD) 18.5, one group of pregnant rats (n = 5) was euthanized by CO_2 asphyxiation followed by cervical dislocation. A longitudinal incision along the entire length of the uterus was made, and the attached placenta was either fixed in 4% buffered formaldehyde (for immunohistochemistry) or embedded in OCT and snap-frozen (for immunofluorescence). Whole placental tissue extracts were prepared to estimate the activities of various AOX proteins.

Immunohistochemistry. IHC was performed using paraffin-embedded sections as reported earlier (Banu et al., 2016). Optical intensity of immunoreactive protein was measured and numerical data were expressed as least square mean ± SEM, P < .05.

Immunofluorescence. The placentas were embedded in OCT (Fisher Healthcare, Houston, Texas) and sections (5 μm) were processed for immunofluorescence. Briefly, the placenta sections were fixed in 2% buffered paraformaldehyde for 15 min at room temperature. After incubation, the sections were washed in PBS 3 times for 5 min and incubated with methanol (prechilled to −20°C) for 10 min. Subsequently, the sections were washed in PBS for 5 min and incubated with blocking buffer (PBS containing 0.3% Triton X-100 and 5% goat serum) for 1 h at room temperature. Then the sections were incubated overnight at 4 °C with rabbit polyclonal antibody specific for cytokeratin. On the following day, the sections were washed in PBS 3 times for and incubated with Alexa Fluor 488-conjugated goat anti-rabbit secondary antibody for 1 h at room temperature. The

sections were washed with PBS and mounted using ProLong Gold antifade reagent with DAPI (Life Technologies, Eugene, Oregon). The slides were kept in the dark overnight at room temperature and images were captured using a Zeiss Axioplan Microscope with an Axiocam HRc color digital camera (Carl Zeiss Microimaging, Inc., Thornwood, New York). Significant was measured at P < .05.

Statistical analysis. Effects of CrVI on various parameters in the placental zones were analyzed and the results are expressed as mean ± SEM. Student t-test was used to compare groups and P values ≤ .05 were considered significant.

RESULTS

Effects of CrVI on Fetal Weight
Treatment with CrVI significantly decreased fetal weight compared with control (Figure 1).

Effects of CrVI on the Invasive TCs in the Placenta
In the rat, as in human, specialized populations of TCs escape from the placenta and invade into the uterine stroma and establish relationships with uterine blood vessels (Rosario et al., 2009). Two populations of invading TCs, namely, interstitial and
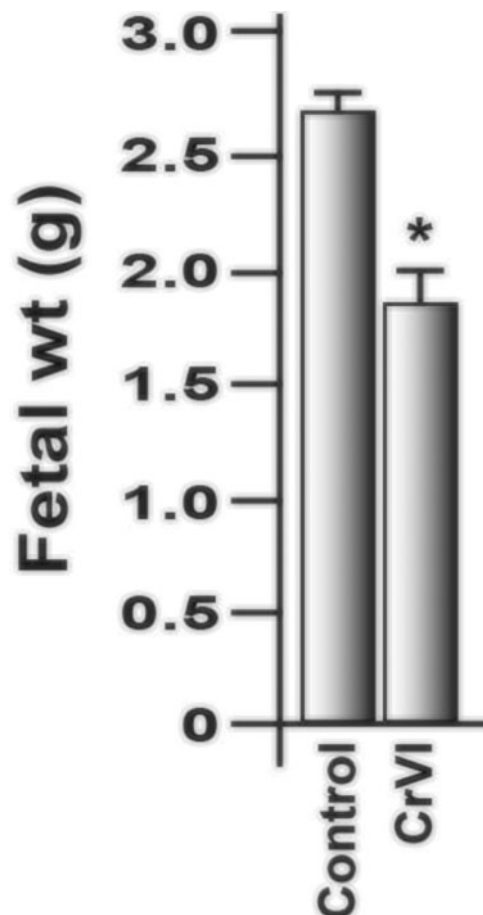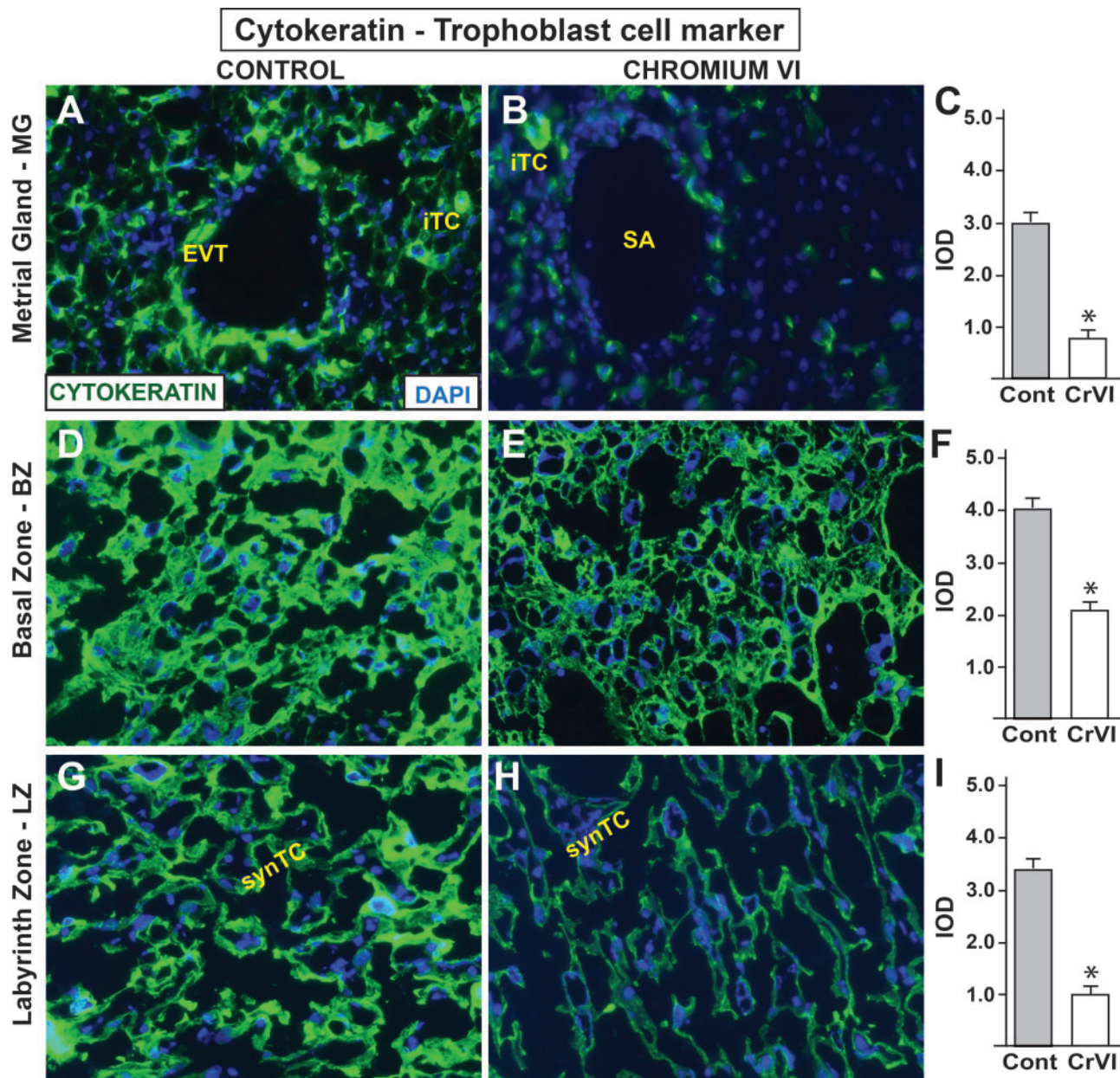

FIG. 1. Effect of CrVI on the fetal weight on 18.5 dpc. Pregnant mothers (n = 5) received drinking water with or without CrVI (50 ppm) from GD 9.5 to 14.5. The rats were euthanized on 18.5 dpc, and fetuses were separated and weighed. CrVI significantly decreased fetal weight (Figure 1). dpc, days postcoitum. Each value represents mean ± SEM of 25 placentas. *Control versus CrVI, P < .05.
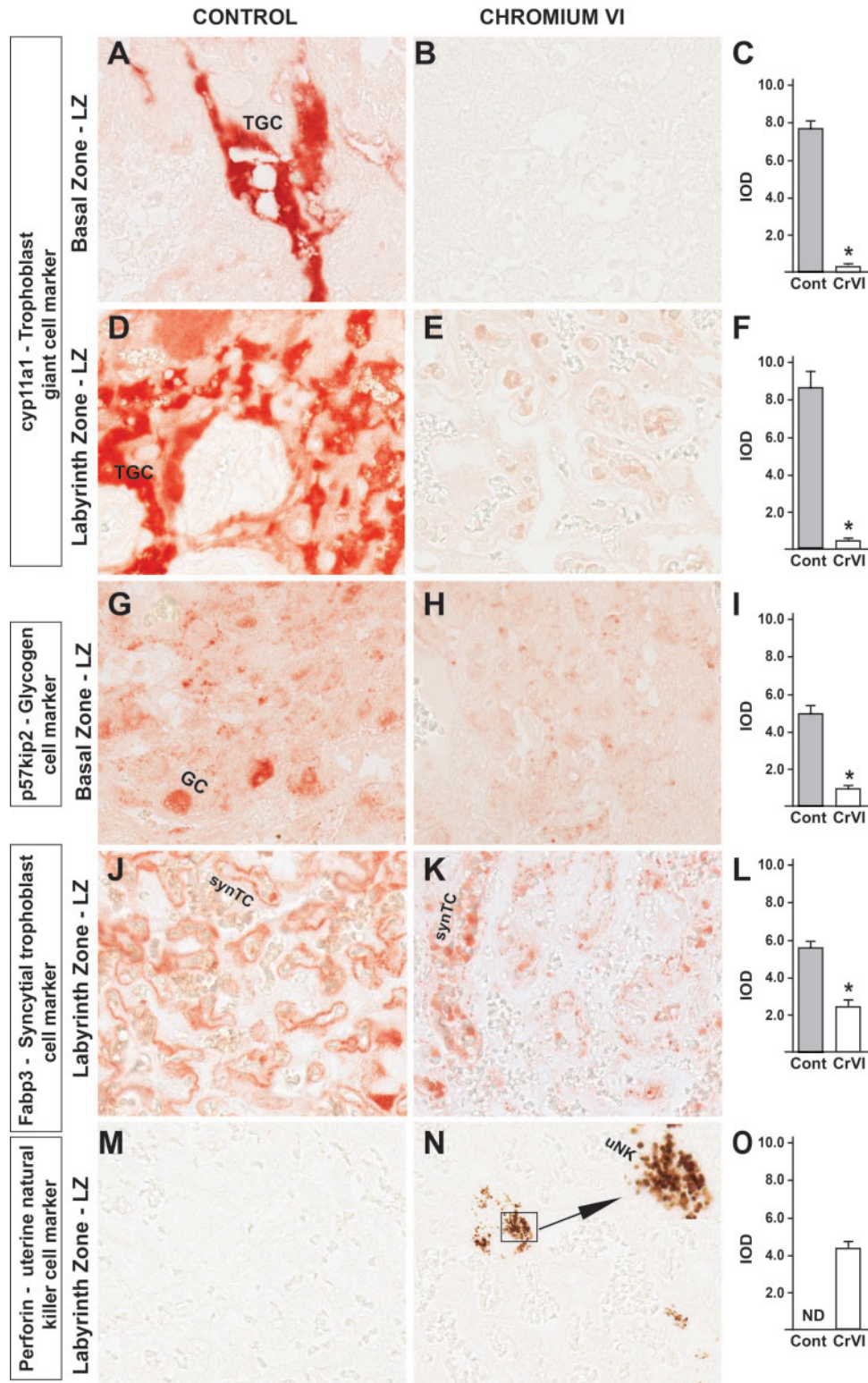
FIG. 2. Effect of CrVI on the expression of TC marker cytokeratin on 18.5 dpc. Pregnant mothers (n = 5) received drinking water with or without CrVI (50 ppm) from 9.5 to 14.5 dpc. Placentas were separated on 18.5 dpc, embedded in OCT and processed for immunofluorescence. Images were captured from MG (**A**, control; **B**, CrVI), BZ (**D**, control; **E**, CrVI), labyrinth zone (**G**, control; **H**, CrVI), and shown in histograms (MG, **C**; BZ, **F**; and LZ, **I**). EVT - endovascular trophoblast, iTC, interstitial trophoblast; SA, spiral artery; synTC, syncytial trophoblast. MG, metrial gland; BZ, basal zone; LZ, labyrinth zone; YS, yolk sac; dpc, days postcoitum. CrVI decreased TCs invasion into the MG. Each value represents mean ± SEM of 5 placentas. *Control versus CrVI, P < .05. Width of field for each image is 220 μm.

endovascular TCs can be identified (Rosario *et al.*, 2009). In order to identify the effects of CrVI on TC population, we performed immunofluorescence staining of TC marker cytokeratin in the placenta and metrial gland (MG). In the control group, invasion of TCs into the endothelial layer of the uterine spiral artery was apparent (Figs. 2A, D, and G). In addition, interstitial TCs were also very well distributed in the smooth muscle layer of the MG. However, CrVI significantly decreased both endovascular and interstitial TC populations in the MG. Basal zone (BZ) from the control placenta was enriched with TCs (Figure 2D), whereas, CrVI-induced decrease in TCs in BZ was highly significant (P ≤ .05) (Figs. 2E and F). The labyrinth zone (LZ) was filled with multinucleated syncytial TCs (synTCs) in control rats (Figure 2G). CrVI significantly decreased synTCs (Figs. 2H and I).

Effects of CrVI on the Distribution of Various TC Lineages

At least 3 major lineages of differentiated trophoblasts are found in the BZ (also called junctional zone), namely, trophoblast giant cells (TGCs), spongiotrophoblast cells (spTCs), and glycogen cells (GCs). In order to identify these cells, we detected these cells with the expression of suggestive (if not definitive) cell-specific markers. Cell-specific proteins and antibodies for the phenotypic analysis of cells within the uteroplacental compartment were chosen based on the protocols from Soares' lab (Ain *et al.*, 2006). Cytochrome p450scc (Cyp11a1) is a TGC marker, whereas, p57kip2 is a GC marker. Notably, TGCs are distributed both in the BZ and LZ of the rat placenta (Peel and Bulmer, 1977). Cytochrome p450scc/Cyp11a1 expression was very high in the BZ and LZ of control rats (Figs. 3A and D). However, there

FIG. 3. Effect of CrVI on the expression of TC differentiation markers of various placental compartments on 18.5 dpc. Pregnant mothers (n = 5) received drinking water with or without CrVI (50 ppm) from 9.5 to 14.5 dpc. Placentas were separated on 18.5 dpc and processed for IHC. Representative images are shown for the expression of the following markers: cyp11a1, TGC marker in the BZ (**A**, Control; **B**, CrVI; and **C**, histogram) and LZ (**D**, Control; **E**, CrVI; and **F**, histogram); p57kip2, GC marker in the LZ (**G**, Control; **H**, CrVI; and **I**, histogram); Fabp3, syncytial trophoblast marker in the LZ (**J**, Control; **K**, CrVI; and **L**, histogram); Perforin, uNK cell marker in the LZ (**M**, Control; **N**, CrVI; and **O**, histogram). The inset **(N)** shows an enlarged view of the infiltration of uNK cells in the synTCs of the LZ. TGC, trophoblastic giant cells; GC, glycogen cells; synTC, syncytial trophoblast; uNK, uterine natural killer cells; BZ, basal zone; LZ, labyrinth zone; dpc, days postcoitum. Each value represents mean ± SEM of 5 placentas. *Control versus CrVI, $P < .05$. Width of field for each image is 220 μm.

was a striking decrease in Cyp11a1 expression with CrVI treatment both in the BZ as well as LZ (Figs. 3B, C, E, and F). Expression of GC marker p57kip2 was also significantly decreased by CrVI compared with control (Figs. 3G–I). Fatty acid-binding protein 3 (Fabp3) is a specific marker for synTCs. CrVI significantly decreased the expression of Fabp3 compared with control, indicating a significant reduction in the population of synTC cells. Uterine natural killer cells (uNKs), are directly involved in the migration of TCs into the uterine stroma and/or myometrium. These are the key immune cells that predominantly populate the pregnant uterus mediating immune tolerance in the maternal-fetal interface. uNK cells were absent in the MG of both control and CrVI-treated rats (data not shown). However, we observed expression of uNKs in the LZ with CrVI treatment, but not in control rats (Figs. 3 M–O).

Effects of CrVI on the Expression of Cyclin D1
Cyclin D1 (Ccnd1) plays a critical role in cell division during G1 phase (Schwartz and Shah, 2005). In control rats, cyclin D1 was expressed in endovascular TCs of the uterine spiral artery (Figure 4A), TGCs of the BZ (Figure 4D), and cytotrophoblast cells of the LZ (Figure 4G). CrVI significantly decreased cyclin D1 expression in MG, BZ and LZ, with no change in yolk sac (YS), compared with control (Figs. 4B, C, E, F, H, and I).

Effects of CrVI on Oxidative Stress and the Activities of AOXs in the Placenta
Whole placental extracts were prepared and oxidative stress markers (LPO and H_2O_2), and AOXs (Gpx1 and Sod) were estimated using kits according to the manufacturer's instruction. CrVI significantly increased LPO and H_2O_2 activities, and decreased AOX activities (Figs. 5A–D).

Effects of CrVI on the Expression of AOX Proteins in the Placenta
Our previous findings in the ovary indicated that CrVI increased ROS and decreased various AOX enzymes (Stanley *et al.*, 2013). Information from the literature shows clear evidence of the increased levels of oxidative stress in placental pathologies including preeclampsia (Jauniaux and Burton, 2016). Heavy metals increase oxidative stress in the human placenta, and an
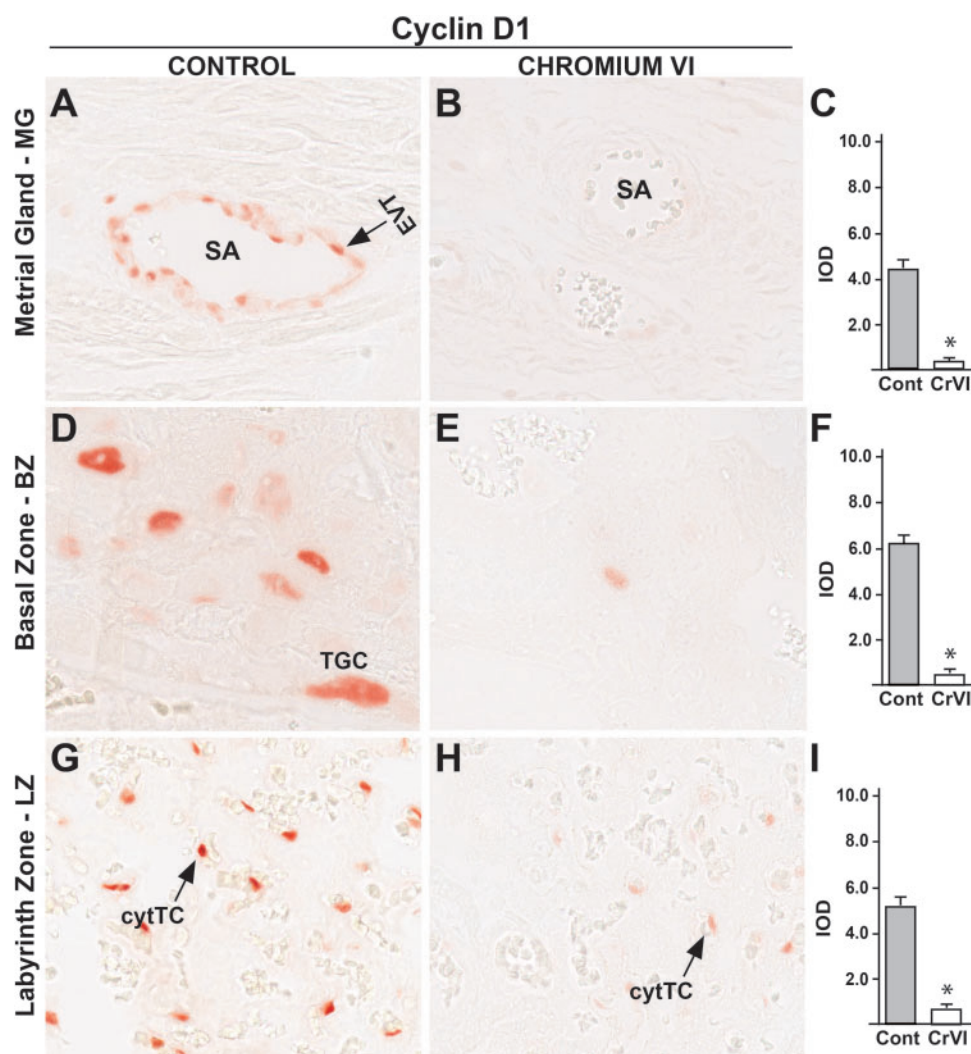

FIG. 4. Effect of CrVI on the expression of cyclin D1 on 18.5 dpc in the placenta. Pregnant mothers (n = 5) received drinking water with or without CrVI (50 ppm) from 9.5 to 14.5 dpc. Placentas were separated on 18.5 dpc and processed for IHC. Representative images are shown for the expression of cyclin D1 in MG (**A**, Control; **B**, CrVI and **C**, histogram) and BZ (**D**, Control; **E**, CrVI; and **F**, histogram); and LZ (**G**, Control; **H**, CrVI, and **I**, histogram). EVT, endovascular trophoblast; SA, spiral artery; TGC, trophoblastic giant cells; cytTC, cytotrophoblast cells; dpc, days postcoitum. Each value represents mean ± SEM of 5 placentas. *Control versus CrVI, P < .05. Width of field for each image is 220 μm.
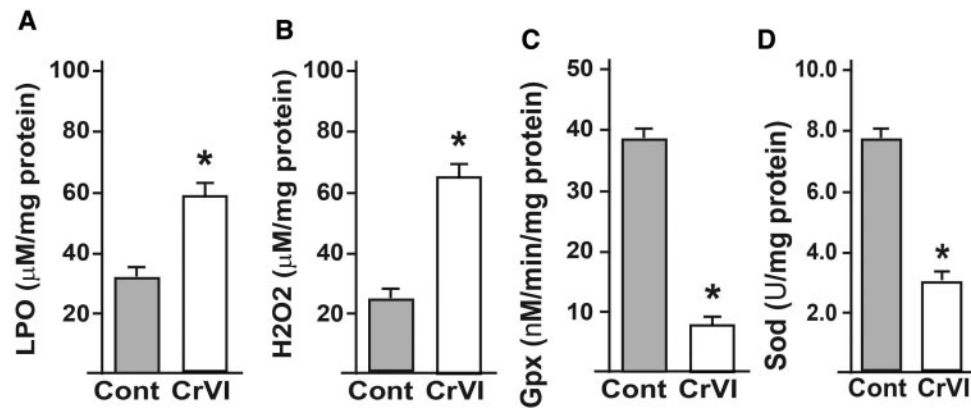
FIG. 5. Effect of CrVI on the activities of oxidative stress markers (LPO and H_2O_2) and AOXs (Gpx and Sod) in the placental extracts. Pregnant mothers (n = 5) received drinking water with or without CrVI (50 ppm) from 9.5 to 14.5 dpc. Placentas were separated on 18.5 dpc and extracts prepared as given in materials and methods. Histograms of LPO (**A**), H2O2 (**B**), Gpx (**C**), and Sod (**D**) are shown. dpc, days postcoitum. Each value represents mean ± SEM of 5 placentas. *Control versus CrVI, $P < .05$.

increase in oxidative stress was directly correlated with the exposure to heavy metals (Serafim *et al.*, 2012). However, there is no clear understanding of the mechanistic aspects of CrVI on placental oxidative stress or AOX status. Therefore, we determined the spatial expression patterns of cytoplasmic (Gpx1 and Sod1) and mitochondrial Sod2, peroxiredoxin (Prdx)-3 and thioredoxin (Txn)-2 AOX enzymes in the placenta.

Gpx1 was expressed in interstitial and endovascular TCs around the spiral arteries in MG, TGCs in BZ, as well as in YS epithelium (Figs. 6A, D, G, and J). CrVI significantly downregulated Gpx1 interstitial and endovascular TCs in MG (Figs. 6B and C), TGCs in BZ (Figs. 6E and F) and YS (Figs. 6K and L) but not in LZ (Figs. 6H and I).

In control rats, Sod1 was seldom expressed in MG (Figs. 7A–C), significantly increased in TGCs in BZ (Figure. 7D), synTCs in LZ (Figure 7G), and in YS epithelium (Figure 7J). CrVI did not change Sod1 expression either in MG (Figs. 7B and C) or in YS (Figs. 7K and L), but it significantly down regulated Sod1 expression TGCs in BZ and synTCs in LZ (Figs. 7E, F, H, and I). Thus Sod1 expression was predominant and specific to the TCs of the BZ and LZ.

Sod2 was expressed in interstitial and endovascular TCs around the spiral arteries in MG (Figure 8A), TGCs of BZ (Figure 8D), cyto- and synTCs in LZ (Figure 8G), and YS epithelium (Figure 8J). Interestingly, CrVI upregulated Sod2 expression in interstitial and endovascular TCs in MG (Figs. 8B and C), down regulated in trophoblastic giant cells of BZ (Figs. 8E and F), synTCs in LZ (Figs. 8H and I) and did not change in YS (Figs. 8K and L), exhibiting a spatial expression pattern, as well as specific expression in TCs.

In control rats, Prdx3 was abundantly expressed in interstitial and endovascular TCs around the spiral arteries in MG (Figure 9A), TGCs in BZ (Figure 9D), cyto- and synTCs in LZ (Figure 9G), and YS epithelium (Figure 9J). CrVI significantly down regulated Prdx3 in interstitial and endovascular TCs in MG, but not in smooth muscle cells (Figure 9B). CrVI decreased Prdx3 in TGCs in BZ (Figure 9E), in cyto- and synTCs in LZ (Figure 9 H), and YS epithelium (Figure 9K).

Txn2 was expressed in interstitial and endovascular TCs around the spiral arteries in MG (Figure 10A). It was high in the GCs in trophoblastic giant cells of BZ, synTCs in LZ, and YS epithelium (Figure 10A, D, G, and J). CrVI significantly down regulated Txn2 in all the trophoblastic cell types (Figs. 10B, C, E, F, H, I, K, and L).

DISCUSSION

Previous findings from our lab indicated that CrVI (25 ppm) exposure during 9.5–14.5 dpc had reduced the litter size, decreased pregnancy outcome, and advanced reproductive senescence in the F1 offspring, resulting in premature ovarian failure (POF) in the F1 offspring (Sivakumar *et al.*, 2014). CrVI-induced POF was mediated through the disruption of Xpnpep-2, a POF marker gene in the human, and its substrates collagens throughout the ovarian development (Banu *et al.*, 2015). Women exposed to CrVI from chrome industries suffer from preterm labor and their children are affected by IUGR (Quansah and Jaakkola, 2008), with an increased levels of Cr in the cord blood (Shmitova, 1980). Exposure of the placenta to adverse chemicals during its development leads to several pregnancy complications and IUGR (Levario-Carrillo *et al.*, 2004; Seidler *et al.*, 1999; Zhang *et al.*, 1992). Therefore, the current study attempts to understand the effects of CrVI on the placenta, in particular on the TCs. A previous finding (Lee *et al.*, 2004) in rat showed that exposure to very high doses of CrVI (250 and 750 ppm) from 7 to 19 dpc suppressed the differentiation of spTCs on 11 dpc, and induced apoptosis of placental cells, reduced placental and fetal weights, and litter size on 20 dpc. This study showed that exposure of pregnant rats to CrVI (50 ppm) through drinking water from 9.5 to 14.5 dpc reduced fetal weight. The dose of CrVI used in the study is environmentally relevant to some of the worst polluted places of the world such as India (Dubey *et al.*, 2001b; Rao *et al.*, 2011), Mexico (Armienta-Hernández and Rodríguez-Castillo, 1995), China (Zhang and Li, 1987), and Bangladesh (Frisbie *et al.*, 2002). Moreover, the pregnancy window of 9.5–14.5 dpc is the active period for TCs proliferation (Jollie, 1964). TCs proliferation slows down after 14.5 dpc. Therefore, we chose the specific window (9.5–14.5 dpc) for CrVI exposure.

TCs arise from the trophectoderm of the developing embryo and are the first committed cell lineage in mammalian development, which eventually differentiate into a multilineage pathway. In order to identify the effects of CrVI on various TC lineages, we immunostained TCs with specific markers. Cytokeratin is a reliable marker for TCs which is expressed throughout the pregnancy (Ain *et al.*, 2006). CrVI decreased TC population in the BZ and LZ. Our recent study indicated that CrVI-induced apoptosis of TCs through casp-3/AIF/p53 pathways (Banu *et al.*, 2016). In some species, including the rat, mouse and human, specialized populations of TCs invade into
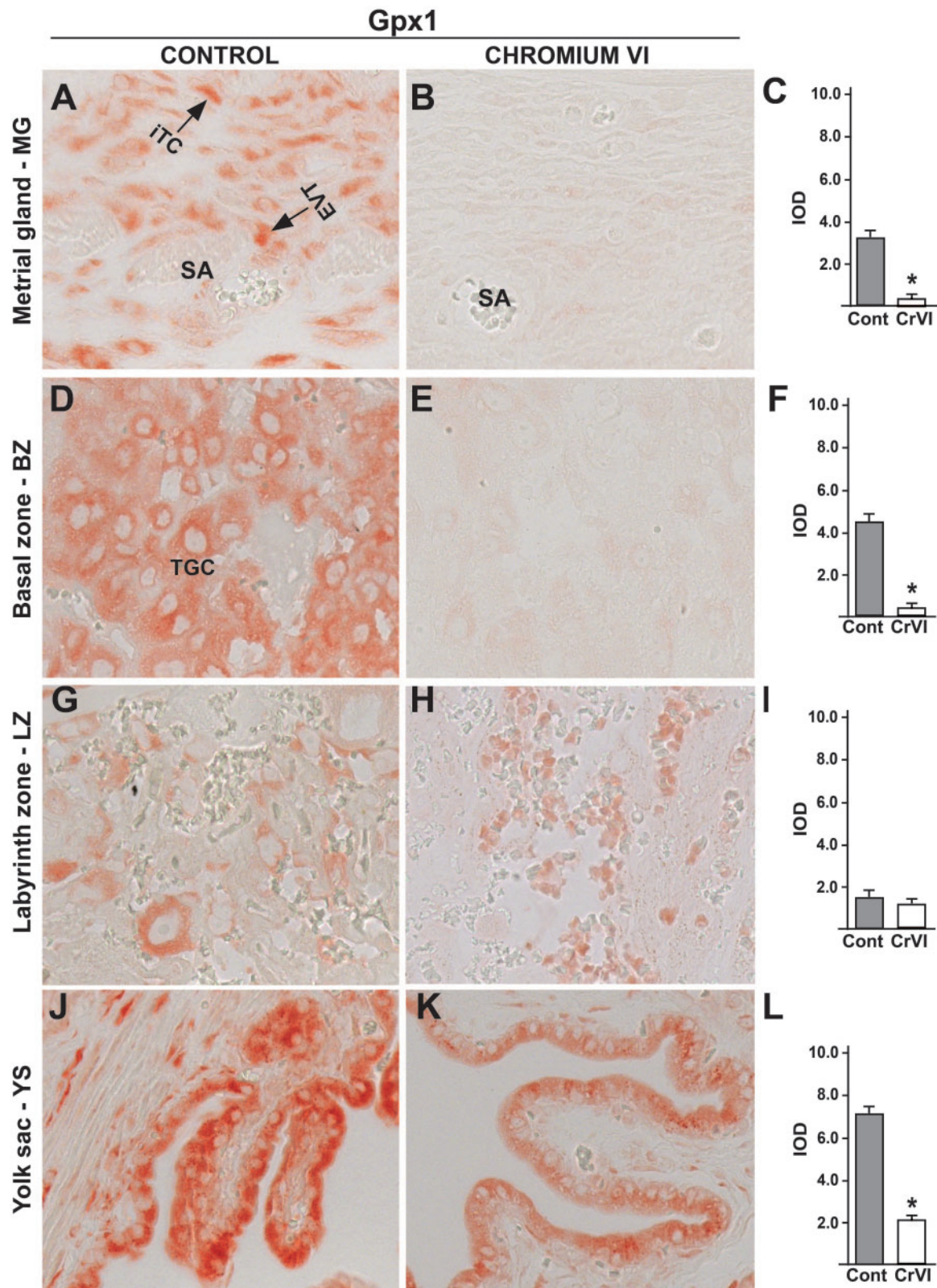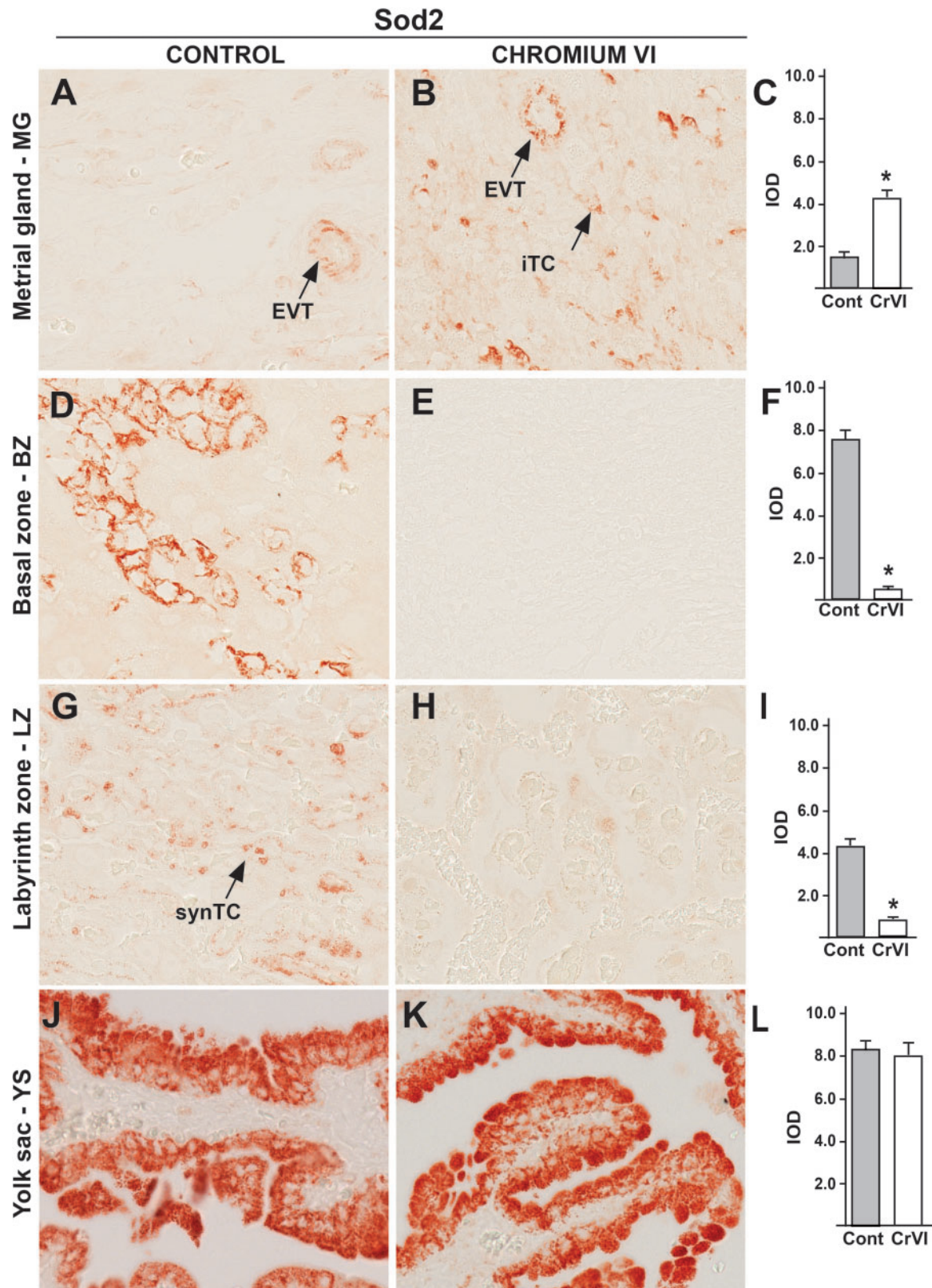
FIG. 6. Effect of CrVI on the expression of Gpx1 on 18.5 dpc in the placenta. Pregnant mothers (n = 5) received drinking water with or without CrVI (50 ppm) from 9.5 to 14.5 dpc. Placentas were separated on 18.5 dpc and processed for IHC. Representative images are shown for the expression of Gpx1 in MG (**A**, Control; **B**, CrVI; and **C**, histogram) and BZ (**D**, Control; **E**, CrVI; and **F**, histogram); LZ (**G**, Control; **H**, CrVI; and **I**, histogram) and YS (**J**, Control; **K**, CrVI; and **L**, histogram). EVT, endovascular trophoblast; iTC, interstitial trophoblast; TGC, trophoblastic giant cells; dpc, days postcoitum. Each value represents mean ± SEM of 5 placentas. *Control versus CrVI, P < .05. Width of field for each image is 220 μm.
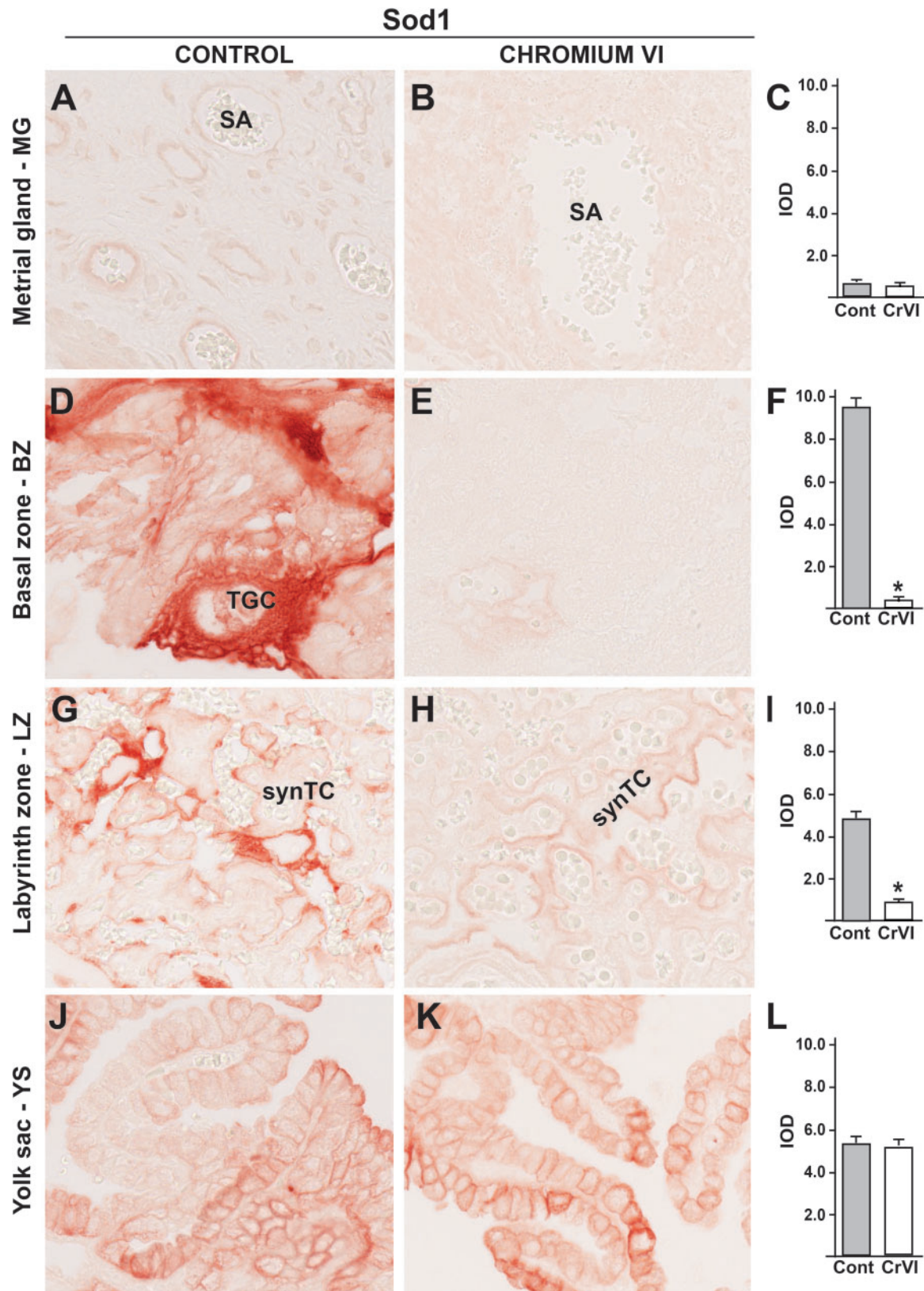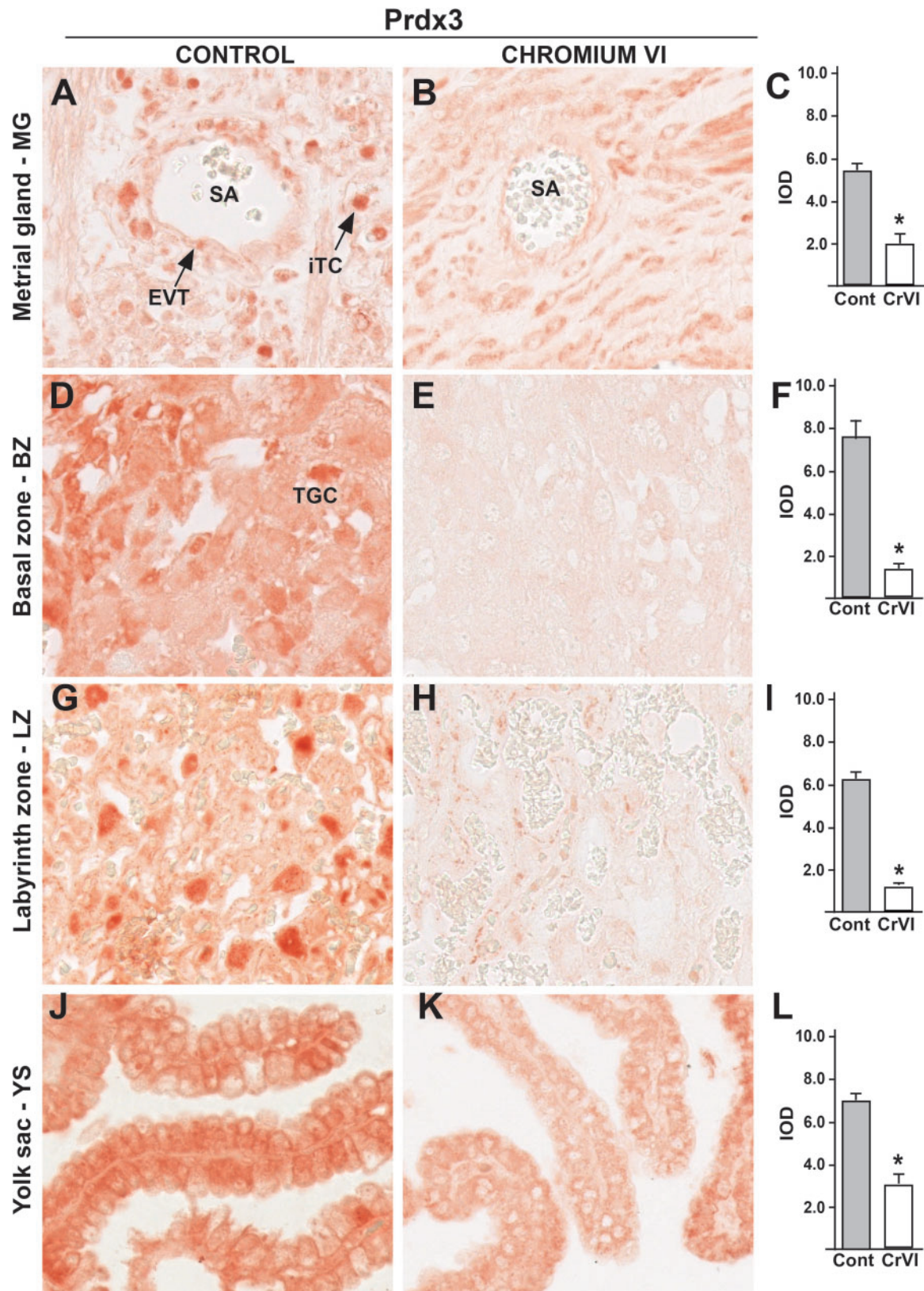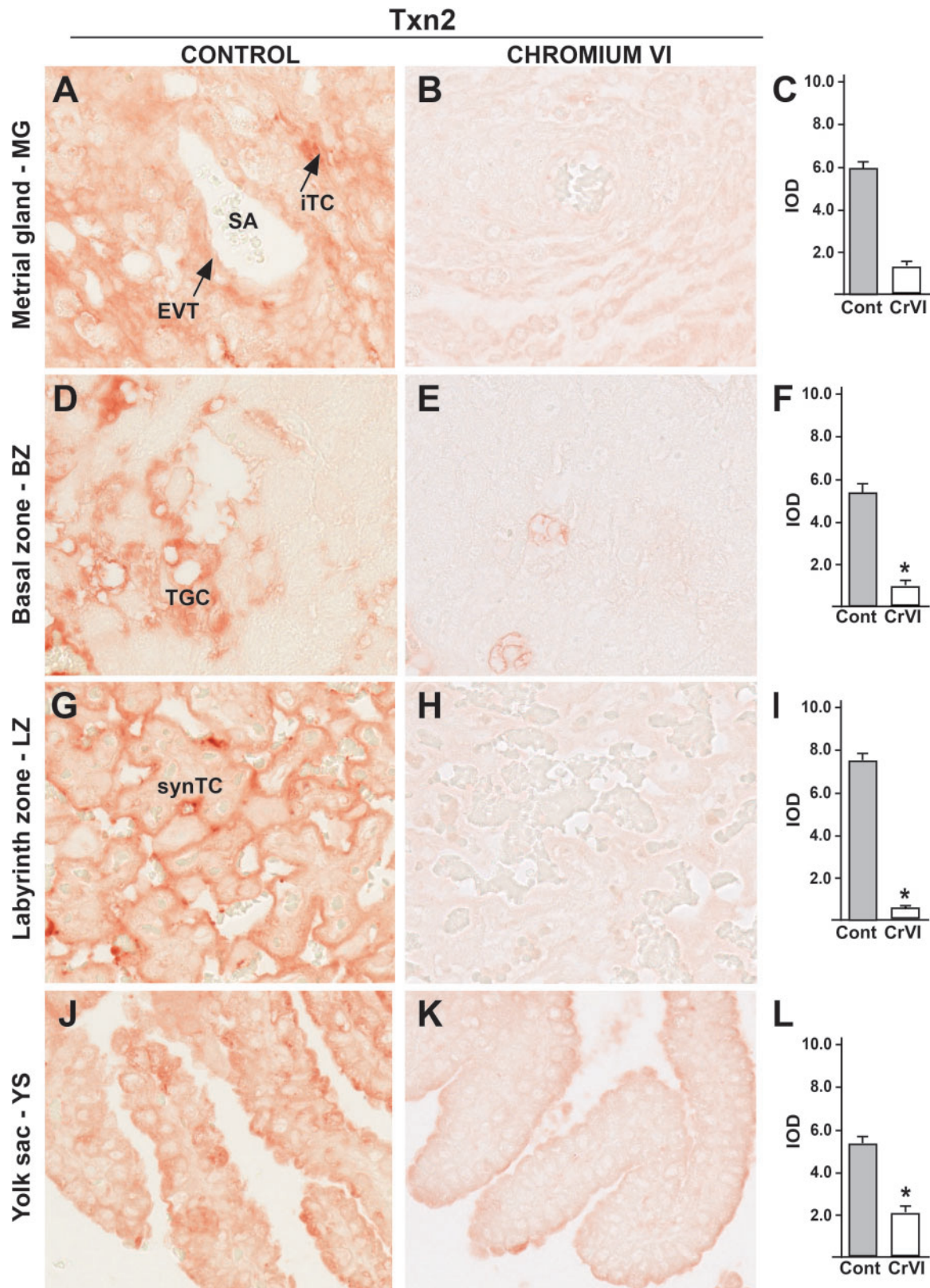
FIG. 7. Effect of CrVI on the expression of Sod1 on 18.5 dpc in the placenta. Pregnant mothers (n = 5) received drinking water with or without CrVI (50 ppm) from 9.5 to 14.5 dpc. Placentas were separated on 18.5 dpc and processed for IHC. Representative images are shown for the expression of Sod1 in MG (**A**, Control; **B**, CrVI; and **C**, histogram) and BZ (**D**, Control; E, CrVI; and **F**, histogram); LZ (**G**, Control; **H**, CrVI; and **I**, histogram) and YS (**J**, Control; **K**, CrVI; and L, histogram). TGC, trophoblastic giant cells; synTC, syncytial trophoblast; dpc, days postcoitum. Each value represents mean ± SEM of 5 placentas. *Control versus CrVI, $P < .05$. Width of field for each image is 220 μm.

FIG. 8. Effect of CrVI on the expression of Sod2 on 18.5 dpc in the placenta. Pregnant mothers (n = 5) received drinking water with or without CrVI (50 ppm) from 9.5 to 14.5 dpc. Placentas were separated on 18.5 dpc and processed for IHC. Representative images are shown for the expression of Sod2 in MG (**A,** Control; **B,** CrVI; and **C,** histogram) and BZ (**D,** Control; **E,** CrVI; and **F,** histogram); LZ (**G,** Control; **H,** CrVI; and **I,** histogram) and YS (**J,** Control; **K,** CrVI; and **L,** histogram). EVT, endovascular trophoblast; iTC, interstitial trophoblast; synTC, syncytial trophoblast; dpc, days postcoitum. Each value represents mean ± SEM of 5 placentas. *Control versus CrVI, P ≤ .05. Width of field for each image is 220 μm.

FIG. 9. Effect of CrVI on the expression of Prdx3 on 18.5 dpc in the placenta. Pregnant mothers (n = 5) received drinking water with or without CrVI (50 ppm) from 9.5 to 14.5 dpc. Placentas were separated on 18.5 dpc and processed for IHC. Representative images are shown for the expression of Prdx3 in MG (**A**, Control; **B**, CrVI; and **C**, histogram) and BZ (**D**, Control; **E**, CrVI; and **F**, histogram); LZ (**G**, Control; **H**, CrVI; and **I**, histogram) and YS (**J**, Control; **K**, CrVI; and **L**, histogram). EVT, endovascular trophoblast; iTC, interstitial trophoblast; SA, spiral artery; TGC, Trophoblastic giant cells. Each value represents mean ± SEM of 5 placentas. *Control versus CrVI, P < .05. Width of field for each image is 220 μm.

FIG. 10. Effect of CrVI on the expression of Txn2 on 18.5 dpc in the placenta. Pregnant mothers (n = 5) received drinking water with or without CrVI (50 ppm) from 9.5 to 14.5 dpc. Placentas were separated on 18.5 dpc and processed for IHC. Representative images are shown for the expression of Txn2 in MG (**A**, Control; **B**, CrVI; and **C**, histogram) and BZ (**D**, Control; **E**, CrVI; and **F**, histogram); LZ (**G**, Control; **H**, CrVI; and **I**, histogram) and YS (**J**, Control; **K**, CrVI; and **L**, histogram). EVT, endovascular trophoblast; iTC, interstitial trophoblast; synTC, syncytial trophoblasts. Each value represents mean ± SEM of 5 placentas. *Control versus CrVI, P < .05. Width of field for each image is 220 µm.

the uterine stroma and induce specific modifications of the uterine blood vessels. The invasive TCs are known as interstitial TCs when they are localized within the uterine stroma. On the other hand, when TCs invade into uterine vasculature (trophoblastic vascular colonization), they are called endovascular TCs. These cells replace the endothelium of the uterine artery and are situated between the vasculature (Rosario et al., 2009). In the human, the invasive TC lineage is referred to as extravillous trophoblast (Velicky et al., 2016). During the latter phase of pregnancy, TC invasive events in the rat are remarkably similar to human TC invasion (Ain et al., 2006; Fonseca et al., 2012). Striking evidence from this study shows that CrVI significantly decreased TC invasion into the MG. Abnormal invasion of TCs and poor uterine artery remodeling adversely affect the establishment of pregnancy, and in severe cases may lead to pregnancy loss or preterm labor. The actual mechanism of CrVI-induced decrease in TC invasion is currently unknown. Our ongoing investigations are expected to identify the mechanism(s).

uNKs are directly involved in the migration of TCs into the uterine stroma and/or myometrium (Sharma, 2014). The dynamics of NK cells in the placentation site during rat pregnancy has been well characterized (Ain et al., 2003). In fact, the invading TCs occupy the locations previously occupied by uNK cells, indicating a regulatory role for uNK cells in TCs invasion (Moffett and Colucci, 2014; Pijnenborg et al., 1981). Synchronization between uNKs, invasive TCs and decidual cells is crucial to produce a suitable environment throughout pregnancy in order to establish an adequate nutrient transfer to the growing embryo. Survival of the allogeneic embryo in the uterus depends on the maintenance of immune tolerance at the maternal-fetal interface. uNKs are the key immune cells that predominantly populate the pregnant uterus. In normal pregnancy, the timing of TC movement into the uterus is precise and coincides with the departure or disappearance of uNK cells. Since CrVI decreased TC invasion into MG and uterine vasculature, we immunostained MG for uNK marker perforin. uNK cells were absent in the MG of both the control and CrVI exposed groups. Early reports in rat placenta indicated that uNK cells are rarely seen or absent in late pregnancy in rats (Fonseca et al., 2012; Soares et al., 2012). Interestingly, CrVI increased uNK cells in the LZ. An extensive review on uNK cells by Sharma (Sharma, 2014) suggests that infiltration of uNK cells into placental zone is an adverse feature in pregnancy. The LPS-induced increase in uNK cells was associated with an increase in NK1.1+ cells which became the potent source of excessive TNF-α at the maternal-fetal interface (Murphy et al., 2005). It was proposed that uNK cells infiltrated into placental zone or fetal-maternal interface have the ability to harm fetal survival directly or by encouraging propagation of other inflammatory immune cells. Thus we propose that CrVI may have induced an infiltration of uNK cells which could be a sign of adverse outcome for the placenta as well as the fetus.

BZ (also known as junctional zone) consists of trophoblastic giant cells, spongiotrophoblasts and GCs. Cyp11a1 (cytochrome p450scc) is a marker for TGCs. p57kip2 is a GC marker (Ain et al., 2006). CrVI decreased both Cyp11a1 and p57kip2, indicating a decrease in the population of GCs and trophoblastic giant cells. CrVI may have decreased the TCs population by increasing TCs apoptosis, decreasing cell proliferation/survival, or by inhibiting trophoblastic stem cell differentiation. Moreover, the very first step in the process of steroidogenesis is the conversion of cholesterol into pregnenolone by Cyp11a1 (Payne and Hales, 2004). CrVI strikingly decreased the expression of Cyp11a1 both in the BZ and LZ, indicating its adverse effects on placental steroidogenesis. LZ consists of cyto- and synTCs. Fabp3 is a marker for synTCs (Ain et al., 2006). CrVI significantly decreased synTCs. Overall, these data along with our recently published data on the outcome of CrVI exposure on TCs apoptosis and cell survival machinery, demonstrate that CrVI decreased TCs proliferation, induced apoptosis and reduces TCs invasion into MG from the placental zones. Further mechanistic studies are needed to delineate the exact mechanism of CrVI in altering the key signaling pathways.

In order to further understand the mechanism of CrVI in causing the above described adverse effects, we determined the oxidative stress markers and AOX proteins in the placenta and MG. Data from this study clearly indicate an adverse effect of CrVI on placental redox balance. Increased oxidative stress is encountered in certain pathologic pregnancies complicated by maternal diabetes, preeclampsia, or early pregnancy loss. This increased oxidative stress can affect placental function, induce pregnancy complications, and decrease birth weight. A recent epidemiological study reported a positive correlation between concentrations of heavy metals such as cadmium and lead and preterm birth in women due to an increase in oxidative stress and decrease in glutathione levels (Singh et al., 2015). A similar study in preeclamptic women showed increased levels of Cd with a concomitant decrease in zinc compared with women with normal pregnancy. Edaravone, a potent ROS scavenger, inhibited hypoxia-induced ROS production and sFlt-1 secretion in immortalized HRT-8 TCs (Zhao et al., 2014). Production of autoantibodies against Prdx family members PRX3 and PRX4 resulted in recurrent spontaneous abortion in women. These autoimmune antibodies against PRX3 and PRX4 were suggested to neutralize their AOX function, thus rendering conceptuses prone to developmental arrest and loss (Gharesi-Fard, 2015). Data from this study showed that CrVI significantly decreased Gpx1, Sod1, Sod2, Prdx3, and Txn2 in placental zones and MG with a single exception of increasing Sod2 in the MG. However, overall activity of total Sod was decreased with CrVI exposure.

Interestingly, we have noticed differences in responses to CrVI-toxicity by various types of TCs compared with YS epithelium. This differential responsiveness is further indicative of greater sensitivities of cell specific regulatory pathways. Additionally, our results also indicate that CrVI toxicity is more specific to trophoblasts (rather than YS epithelium or uterine smooth muscle cells), and it is also differential based on the protein and/or the pathway studied, which is biologically and toxicologically more interesting. Thus, this study suggests that CrVI-induced adverse effects on the placenta may be mediated through multiple mechanisms. Based on the data from the current study we suggest that CrVI-induced increase in ROS and decrease in AOXs may be one of the mechanisms which may potentially affect fetal and placental growth and development that lead to a decrease in fetal weight.

REFERENCES

Ahamed, M., Mehrotra, P. K., Kumar, P., and Siddiqui, M. K. J. (2009). Placental lead-induced oxidative stress and preterm delivery. *Environ. Toxicol. Pharmacol.* **27**, 70–74.

Ain, R., Canham, L. N., and Soares, M. J. (2003). Gestation stage-dependent intrauterine trophoblast cell invasion in the rat and mouse: Novel endocrine phenotype and regulation. *Dev. Biol.* **260**, 176–190.

Ain, R., Konno, T., Canham, L. N., and Soares, M. J. (2006). Phenotypic analysis of the rat placenta. In *Placenta and Trophoblast: Methods and Protocols Volume 1* (M. J. Soares, and J. S. Hunt, Eds.), pp. 295–313. Humana Press, Totowa, NJ.

Andrews, D. (2016). Erin Brockovich carcinogen in tap water of more than 200 million Americans. *Environmental Working Group* 1-13. Available at: https://static.ewg.org/reports/2016/chromium6/EWG_Chrome6Report_C06.pdf.

Annangi, B., Bonassi, S., Marcos, R., and Hernández, A. (2016). Biomonitoring of humans exposed to arsenic, chromium, nickel, vanadium, and complex mixtures of metals by using the micronucleus test in lymphocytes. *Mut. Res.* doi: http://dx.doi.org/10.1016/j.mrrev.2016.03.003.

Armienta-Hernandez, A., and Rodriguez-Castillo, R. (1995). Environmental exposure to chromium compounds in the valley of Leon, Mexico. *Environ. Health Perspect.* **103**, 47–51.

Armienta-Hernández, M. A., and Rodríguez-Castillo, R. (1995). Environmental exposure to chromium compounds in the valley of León, México. *Environ. Health Perspect* **103(Suppl 1)**, 47.

Banu, S. K. (2013). Heavy metals and the ovary. In *Ovarian Toxicology* (P. B. Hoyer, Ed.), 2nd ed., pp. 191–228. CRC Press, Boca Raton, FL.

Banu, S. K., Stanley, J. A., Sivakumar, K. K., Arosh, J. A., Barhoumi, R., and Burghardt, R. C. (2015). Identifying a novel role for X-prolyl aminopeptidase (Xpnpep) 2 in CrVI-induced adverse effects on germ cell nest breakdown and follicle development in rats. *Biol. Reprod.* **92**, 67.

Banu, S. K., Stanley, J. A., Sivakumar, K. K., Arosh, J. A., Taylor, R. J., and Burghardt, R. C. (2016). Chromium VI - Induced developmental toxicity of placenta is mediated through spatio-temporal dysregulation of cell survival and apoptotic proteins. *Reprod. Toxicol.* **16**, 30263–30265.

Barceloux, D. G. (1999). Chromium. *J. Toxicol. Clin. Toxicol.* **37**, 173–194.

Das, A. P., and Mishra, S. (2008). Hexavalent chromium (VI): Environment pollutant and health hazard. *J. Environ. Res. Dev.* **2**, 386–392.

De Rijk, E. P., Van Esch, E., and Flik, G. (2002). Pregnancy dating in the rat: Placental morphology and maternal blood parameters. *Toxicol. Pathol.* **30**, 271–282.

Dubey, C., Sahoo, B., and Nayak, N. (2001a). Chromium (VI) in waters in parts of Sukinda chromite valley and health hazards, Orissa, India. *Bull. Environ. Contam. Toxicol.* **67**, 541–548.

Dubey, S. C., Sahoo, K. B., and Nayak, R. N. (2001b). Chromium (VI) in waters in parts of Sukinda chromite valley and health hazards, Orissa, India. *Bull. Environ. Contam. Toxicol.* **67**, 541–548.

Fonseca, B. M., Correia-da-Silva, G., and Teixeira, N. A. (2012). The rat as an animal model for fetoplacental development: A reappraisal of the post-implantation period. *Reprod. Biol.* **12**, 97–118.

Frisbie, S. H., Ortega, R., Maynard, D. M., and Sarkar, B. (2002). The concentrations of arsenic and other toxic elements in Bangladesh's drinking water. *Environ. Health Perspect.* **110**, 1147–1153.

Gharesi-Fard, B. (2015). Preoxiredoxin family members (Prx3 and Prx4) and pregnancy disorder (recurrent pregnancy loss). *Methods Mol. Biol.* **1208**, 299–311.

Gundacker, C., and Hengstschlager, M. (2012). The role of the placenta in fetal exposure to heavy metals. *Wien Med. Wochenschr.* **162**, 201–206.

Hemminki, K., Kyyronen, P., Niemi, M. L., Koskinen, K., Sallmen, M., and Vainio, H. (1983). Spontaneous abortions in an industrialized community in Finland. *Am. J. Public Health* **73**, 32–37.

Jauniaux, E., and Burton, G. J. (2016). The role of oxidative stress in placental-related diseases of pregnancy. *J. Gynecol. Obstet. Biol. Reprod. (Paris)* **45**, 775–785.

Jollie, W. P. (1964). Radioautographic observations on variations in desoxyribonucleic acid synthesis in rat placenta with increasing gestational age. *Am. J. Anat.* **114**, 161–171.

Jomova, K., and Valko, M. (2011). Advances in metal-induced oxidative stress and human disease. *Toxicology* **283**, 65–87.

Junaid, M., Hashmi, M. Z., Malik, R. N., and Pei, D. S. (2016). Toxicity and oxidative stress induced by chromium in workers exposed from different occupational settings around the globe: A review. *Environ. Sci. Pollut. Res.* **23**, 20151–20167.

Lee, H., Chun, J. H., Moon, D. H., Lee, C. U., Kang, S. G., Son, B. C., Kim, D. H., Lee, C. H., Kim, J. W., and Lee, C. K. (2004). Effects of chromium (VI) exposure on the placental function and reproduction in rats. *J. Prev. Med. Public Health* **37**, 157–165.

Levario-Carrillo, M., Amato, D., Ostrosky-Wegman, P., González-Horta, C., Corona, Y., and Sanin, L. H. (2004). Relation between pesticide exposure and intrauterine growth retardation. *Chemosphere* **55**, 1421–1427.

Lewis, R., Cleal, J., and Hanson, M. A. (2012). Review: Placenta, evolution and lifelong health. *Placenta* **33**, S28–S32.

Li, Y., Xu, X., Liu, J., Wu, K., Gu, C., Shao, G., Chen, S., Chen, G., and Huo, X. (2008). The hazard of chromium exposure to neonates in Guiyu of China. *Sci. Total Environ.* **403**, 99–104.

Liu, K. J., and Shi, X. (2001). In vivo reduction of chromium (VI) and its related free radical generation. *Mol. Cell. Biochem.* **222**, 41–47.

Moffett, A., and Colucci, F. (2014). Uterine NK cells: Active regulators at the maternal-fetal interface. *J. Clin. Invest.* **124**, 1872–1879.

Murphy, S. P., Fast, L. D., Hanna, N. N., and Sharma, S. (2005). Uterine NK cells mediate inflammation-induced fetal demise in IL-10-null mice. *J. Immunol.* **175**, 4084–4090.

Myatt, L. (2010). Reactive oxygen and nitrogen species and functional adaptation of the placenta. *Placenta* **31(Suppl)**, S66–S69.

Notarachille, G., Arnesano, F., Calò, V., and Meleleo, D. (2014). Heavy metals toxicity: Effect of cadmium ions on amyloid beta protein 1–42. Possible implications for Alzheimer's disease. *BioMetals* **27**, 371–388.

Ottenwaelder, H., Wiegand, H., and Bolt, H. (1988). Uptake of 51 Cr (VI) by human erythrocytes: Evidence for a carrier-mediated transport mechanism. *Sci. Total Environ.* **71**, 561–566.

Payne, A. H., and Hales, D. B. (2004). Overview of steroidogenic enzymes in the pathway from cholesterol to active steroid hormones. *Endocr. Rev.* **25**, 947–970.

Peel, S., and Bulmer, D. (1977). Proliferation and differentiation of trophoblast in the establishment of the rat chorio-allantoic placenta. *J. Anat.* **124**, 675–687.

Pellerin, C., and Booker, S. M. (2000). Reflections on hexavalent chromium: Health hazards of an industrial heavyweight. *Environ. Health Perspect.* **108**, A402–A407.

Pijnenborg, R., Robertson, W. B., Brosens, I., and Dixon, G. (1981). Trophoblast invasion and the establishment of haemochorial placentation in man and laboratory animals. *Placenta* **2**, 71–91.

Quansah, R., and Jaakkola, J. J. K. (2008). Paternal and maternal exposure to welding fumes and metal dusts or fumes and adverse pregnancy outcomes. *Int. Arch. Occup. Environ. Health* **82**, 529–537.

Rao, G. T., Rao, V. G., Ranganathan, K., Surinaidu, L., Mahesh, J., and Ramesh, G. (2011). Assessment of groundwater contamination from a hazardous dump site in Ranipet, Tamil Nadu, India. *Hydrogeol. J.* **19**, 1587–1598.

Rosario, G. X., Ain, R., Konno, T., and Soares, M. J. (2009). Intrauterine fate of invasive trophoblast cells. *Placenta* **30**, 457–463.

Schwartz, G. K., and Shah, M. A. (2005). Targeting the cell cycle: A new approach to cancer therapy. *J. Clin. Oncol.* **23**, 9408–9421.

Seidler, A., Raum, E., Arabin, B., Hellenbrand, W., Walter, U., and Schwartz, F. W. (1999). Maternal occupational exposure to chemical substances and the risk of infants small-for-gestational-age. *Am. J. Indus. Med.* **36**, 213–222.

Serafim, A., Company, R., Lopes, B., Rosa, J., Cavaco, A., Castela, G., Castela, E., Olea, N., and Bebianno, M. J. (2012). Assessment of essential and nonessential metals and different metal exposure biomarkers in the human placenta in a population from the south of Portugal. *J. Toxicol. Environ. Health A* **75**, 867–877.

Shanker, A. K., and Venkateswarlu, B. (2011). Chromium: Environmental pollution, health effects and mode of action. In *Encyclopedia of Environmental Health* (J. O. Nriagu, Ed.) Elsevier Publishers, Burlington.

Sharma, P., Bihari, V., Agarwal, S. K., Verma, V., Kesavachandran, C. N., Pangtey, B. S., Mathur, N., Singh, K. P., Srivastava, M., and Goel, S. K. (2012). Groundwater contaminated with hexavalent chromium [Cr (VI)]: A health survey and clinical examination of community inhabitants (Kanpur, India). *PLoS One* **7**, e47877.

Sharma, S. (2014). Natural killer cells and regulatory T cells in early pregnancy loss. *Int. J. Dev. Biol.* **58**, 219–229.

Shmitova, L. A. (1980). Content of hexavalent chromium in the biological substrates of pregnant women and puerperae engaged in the manufacture of chromium compounds. *Gig. Tr. Prof. Zabol.* 33–35.

Sies, H. (1997). Oxidative stress: Oxidants and antioxidants. *Exp. Physiol.* **82**, 291–295.

Singh, L., Agarwal, P., Anand, M., and Taneja, A. (2015). Toxic and essential metals in placenta and its relation with lipid peroxides/glutathione status in pre-term and full-term deliveries. *Asian J. Med. Sci.* **7**, 34–39.

Sivakumar, K. K., Stanley, J. A., Arosh, J. A., Pepling, M. E., Burghardt, R. C., and Banu, S. K. (2014). Prenatal exposure to chromium induces early reproductive senescence by increasing germ cell apoptosis and advancing germ cell cyst breakdown in the F1 offspring. *Dev. Biol.* **388**, 22–34.

Soares, M. J., Chakraborty, D., Rumi, M. A. K., Konno, T., and Renaud, S. J. (2012). Rat placentation: An experimental model for investigating the hemochorial maternal-fetal interface. *Placenta* **33**, 233–243.

Stanley, J. A., Sivakumar, K. K., Nithy, T. K., Arosh, J. A., Hoyer, P. B., Burghardt, R. C., and Banu, S. K. (2013). Postnatal exposure to chromium through mother's milk accelerates follicular atresia in F1 offspring through increased oxidative stress and depletion of antioxidant enzymes. *Free Radic. Biol. Med.* **61C**, 179–196.

Stern, R. M., Berlin, A., Fletcher, A., Hemminki, K., Jarvisalo, J., and Peto, J. (1986). International conference on health hazards and biological effects of welding fumes and gases. *Int. Arch. Occup. Environ. Health* **57**, 237–246.

USEPA. (2009). National primary drinking water regulations. In *EPA 816-F-09-004*, pp. 1–6. United States Environmental Protection Agency, Washington, DC.

Valko, M., Morris, H., and Cronin, M. T. (2005). Metals, toxicity and oxidative stress. *Curr. Med. Chem.* **12**, 1161–1208.

Velicky, P., Knöfler, M., and Pollheimer, J. (2016). Function and control of human invasive trophoblast subtypes: Intrinsic vs. maternal control. *Cell Adh. Migr.* **10**, 154–162.

Walentin, K., Hinze, C., Werth, M., Haase, N., Varma, S., Morell, R., Aue, A., Potschke, E., Warburton, D., Qiu, A., et al. (2015). A Grhl2-dependent gene network controls trophoblast branching morphogenesis. *Development* **142**, 1125–1136.

Yang, Y., Liu, H., Xiang, X. H., and Liu, F. Y. (2013). Outline of occupational chromium poisoning in China. *Bull. Environ. Contam. Toxicol.* **90**, 742–749.

Zhang, J., Cai, W. W., and Lee, D. J. (1992). Occupational hazards and pregnancy outcomes. *Am. J. Ind. Med.* **21**, 397–408.

Zhang, J., and Li, X. (1987). Chromium pollution of soil and water in Jinzhou. *Zhonghua Yu Fang Yi Xue Za Zhi* **21**, 262.

Zhao, Y., Zheng, Y. F., Luo, Q. Q., Yan, T., Liu, X. X., Han, L., and Zou, L. (2014). Edaravone inhibits hypoxia-induced trophoblast-soluble Fms-like tyrosine kinase 1 expression: A possible therapeutic approach to preeclampsia. *Placenta* **35**, 476–482.